RevMexAA (Serie de Conferencias), **16**, 173–188 (2003)

SCIENCE WITH TUNABLE FILTERS

J. Bland-Hawthorn
Anglo–Australian Observatory, New South Wales, Australia

RESUMEN

Dentro de dos años, el filtro sintonizable de OSIRIS en el telescopio GTC de 10 m abrirá una nueva era en imagen espectroscópica, desde 350 nm a 1 micra. Como su antecesor, el TTF en el AAT, OSIRIS va a ofrecer una amplia variedad de modos de observación, asociados al movimiento de carga en el detector, para conseguir imagen diferencial de alta calidad. En algunos casos, simplemente la mera repetición de muchos programas científicos llevados a cabo en el AAT conducirá a avances en varios campos, lo que se conseguirá con la combinación de las mejorías en instrumentación, condiciones de observación y apertura. Por tanto, la mayor sensibilidad prevista conduce a nuevos proyectos: mapas amplios de fuentes extensas, imagen en líneas de absorción, series temporales e imagen coronográfica, por citar sólo unos pocos. OSIRIS conseguirá realizar algunas de las imágenes más profundas de luz difusa hasta la fecha, mucho mejores de las que se pueden conseguir con espectrógrafos de campo integral, y con mayor campo de visión.

ABSTRACT

In just two years, the OSIRIS tunable filter spectrograph on the 10 m GTC will herald a new era in spectrophotometric imaging, from 350 nm to 1 μm. Like its forebear, the TTF at the Anglo–Australian Telescope (AAT), OSIRIS will offer a wide variety of observing modes linked to charge shuffling in order to achieve exquisite differential imaging. In some respects, simply repeating the many science cases conducted at the AAT will lead to advances in a number of fields. This is all but guaranteed by the better apparatus, observing conditions and larger aperture. However, the expected improvement in sensitivity suggests many new avenues: large surveys of extended sources, absorption line imaging, time series and coronographic imaging, to name a few. OSIRIS will provide some of the deepest photometric "diffuse light" images to date, much better than what can be achieved with an integral field spectrograph, and over a much wider field of view.

Key Words: **INSTRUMENTATION: SPECTROGRAPHS — METHODS: OBSERVATIONAL**

1. INTRODUCTION

In 1998, J. Cepa (IAC), J. González (UNAM), and I first began to consider what sort of instrument would provide the GTC with a unique facility. Based on the Anglo–Australian Telescope (AAT) and William Herschel Telescope (WHT) experience, it was clear that the prospect of tuning to an arbitrary spectral band anywhere over the 350 nm to 1 μm window would provide the GTC with an extraordinary spectrophotometric facility. The OSIRIS tunable imaging/multislit spectrograph was approved as the first-light instrument the following year. The instrument was introduced in the SPIE proceedings (Cepa et al. 2000; Cepa et al., this volume, p. 000). All aspects of the instrument have a strong lineage in the Taurus Tunable Filter (TTF) and Multislit Spectrograph at the AAT. A particularly exciting feature of OSIRIS is that it will make use of the many band-switching and "nod & shuffle" modes developed at the AAT since 1994.

Here we do not discuss the technical aspects of tunable imaging. –see the Appendix. There is no such thing as a perfect tunable filter, i.e., a tunable top-hat bandpass of arbitrary bandpass and centroid wavelength (Bland-Hawthorn 2000). The major advantage of tunable filters over monolithic filters, is the ability to calibrate to very high precision any departures from the ideal. All conventional interference filters undergo bandpass degradation (focal plane) or phase shifts over the field (pupil) but these cannot be calibrated for at the telescope.

Tunable imaging filters have made important advances in several astrophysical arenas. These can be broadly divided into two categories: detailed studies of individual extended sources in absorption and emission; wide field multiobject spectroscopy of compact sources. We include here (Section 5 ff.) a review of the first five years of TTF observing (1995–2000). It is evident that simply repeating some of these science cases under better site conditions on a 10 m class telescope will lead to important advances.

In summary, tunable filters are very effective in measuring star formation properties in many different galaxy environments, particularly in clusters and in dense filaments. For surveys of line-emitting sources, tunable filters are close to ideal since object selection is based on what is being measured, e.g., the strength of the Hα line. In this respect, OSIRIS has been correctly labeled the "star formation machine" for extragalactic work.

Tunable filters also provide accurate photometry and object morphologies over the widest possible field. These capabilities are well suited to the study of energetic processes which are expected or known to produce detectable diffuse optical/IR line emission (in order of decreasing energy): colliding clusters; cooling flows; gamma ray bursts, quasars (QSOs), radio galaxies and ultraluminous IR galaxies (ULIRGs), galaxy mergers, QSO/ULIRG jets and winds, AGN and starbursts, hypernovae, supernovae, compact X-ray sources, and so on. There exists a wide class of exotic possibilities including flash photoionization events, galaxy bow shocks, and so forth.

2. IMPORTANCE OF DIFFERENTIAL MEASUREMENT

Differential measurement is of paramount importance in all applied sciences, including astronomy, for one simple reason: systematic error is the fundamental limit to an experimental observation. This leads to a key conclusion. Whenever possible, all experiments should be set up so that the quantity being measured arises from a comparison between two measurables, obtained simultaneously, or almost simultaneously, with the same apparatus (i.e., identical light paths). Freeman Dyson (1999) has argued that modern science began in 1732 when James Bradley was able to demonstrate stellar aberration with a differential method that allowed him to quote measurement accuracies to better than 1 part in 10^5. Bradley's measurement of the speed of light was within 1% of the value derived by Michelson a century later in another differential experiment.

There are numerous examples of differential measurement in astronomy. The *Hipparcos* astrometric satellite mission measures simultaneous positions to stars a fixed angle apart; the *DIVA*, *FAME*, and *Gaia* astrometric missions all plan to use this technique. The planet search experiments achieve an accuracy of 3 m s^{-1} by observing the light of the target star through iodine in gaseous form; this imprints a well calibrated high resolution spectrum on the stellar continuum.

The Sloan Digital Sky Survey (Gunn et al. 1998), which undertakes near-simultaneous drift scanning of the sky in the $u'g'r'i'z'$ bands, achieves photometric colors with an order of magnitude higher precision than what was possible in earlier wide field surveys. The best polarimeters are constructed so that the incident light is sampled in two orthogonal planes, which removes many possible sources of systematic error in the derived Stokes parameters.

There are many other optical/IR techniques (e.g., adaptive optics, time series, integral fields) which have important differential elements to them. We highlight one of particular relevance to OSIRIS. A key application of differential measurement is the "nod & shuffle" technique in order to achieve accurate sky subtraction (Glazebrook & Bland-Hawthorn 2001). This is notoriously difficult to do in the optical and is the major source of systematic error in many published astronomical results. Glazebrook and Bland-Hawthorn have already achieved sky subtraction to much better than 1 part in 10^3, which is some sort of a record for ground-based astronomical spectroscopy! Telescope nodding has a long history in the IR; it is surprising that it has taken so long to be adopted at optical wavelengths.

Some of the most impressive differential experiments arise in radio astronomy. The microwave background experiments interleave observations of the sky with an accurately calibrated and stable bolometer, and are able to detect temperature variations of 1 part in 10^6. One of the most impressive methods is phase referencing with radio interferometers: within a decade, it will be possible to detect the proper motions of all galaxies in the Local Group (Brunthaler et al. 2002).

Differential techniques can greatly suppress correlated noise (e.g., fixed pattern noise due to the CCD read out, or CCD fringing caused by atmospheric telluric features). This can never be true for uncorrelated noise, by definition. In the differenced signals, the noise remains. *However*, if the systematic error approaches zero, it should be possible to observe the same source for many week, months, or even years, before any semblance of systematics can be detected. This argues for differential techniques on the largest telescopes available. It is sometimes alleged that the first few years of the operation of a new telescope is taken up with observations of a few hours or less. But, surely, the major gains must come from combining signals over many nights if the telescope is to break genuinely new ground. This may be a reflection of the poor systematics which haunt most modern instruments.

Science with the GTC 10-m Telescope (Granada, España, 5-8 febrero 2002)
Editors: José Miguel Rodríguez Espinosa, Francisco Garzón López & Verónica Melo Martín

3. DIFFERENTIAL OBSERVING MODES

3.1. *Narrow band on/off switching and charge shuffling*

This constitutes the basic observing mode of tunable filters. A spectral band is observed on the upper part of the chip, and an off-band or a comparison band is observed on the lower part of the chip. This operation is beautifully illustrated by Jones (2001b).

It is normal practice to optimize the on-line bandpass to accommodate the line dispersion while suppressing the sky background. A tunable filter SNR calculator is useful for optimizing this band.[1] The off-band frequency can be chosen to match the night sky contribution in the on-band. In this way, temporal variations in atmospheric transmission are shared equally between each passband over the entire exposure time.

Multiple frequencies can be imaged in a single frame, the number, n, of which is entirely arbitrary. If the detector shuffle dimension has p rows and q columns, say, the field of view of each image in an n-shuffle is $p/(2n-1)$ rows in the vertical direction, and normally the full horizontal extent of q columns.

3.2. *Filter switching and charge shuffling*

OSIRIS has two filter wheels which will hold a large number of filters (Cepa et al., this volume, p. 13). The filter wheels can be operated sufficiently quickly that differential imaging can be obtained between two or more monolithic filters, or between a filter and the tunable filter. This allows for smaller photometric errors between two or more bands, as we discuss in Section 4.

3.3. *Broad–narrow shuffling*

A key advance incorporated into the OSIRIS tunable filters is the ability to choose a narrow bandpass for the on-band line and a much broader bandpass (factor of 4–5) for the off-band image so that we incur only a 20% overhead for the off-band image. Once again (Section 3.1), multiple frequencies can be imaged in a single frame.

3.4. *Straddle shuffle imaging*

When imaging spectral lines that fall on a steeply rising or bright continuum, a powerful feature is the ability to shuffle between on and off bands but where the off band is alternated between two or more frequencies either side of the on-band frequency. This can be used to average out gradients in the spectral response of the CCD, atmosphere, blocking filter, or even the celestial source.

[1] For example, www.aao.gov.au/cgi-bin/ttf.

This is a very useful mode which recognizes the fact that a suitable “off” band cannot always be obtained at a single wavelength. This is now the most widely used observing mode with TTF. A very good example (Section 10) involves accurate continuum subtraction, particularly when looking for weak emission set against a bright source (e.g., traces of ionized gas at the cores of ellipticals).

3.5. *Nod & shuffle imaging*

This technique requires that the telescope is nodded rapidly between targets and adjacent sky positions; the on and off fields are recorded on adjacent regions the CCD with charge shuffling. In Section 3.1 above, we mentioned the importance of optimizing the bandpass to suppress the sky background. In fact, this is particularly important in the presence of a bright night sky line, or absorption lines due to moonlight, both of which can cause serious fringing over the CCD. Nod & shuffle is very effective at reducing fixed pattern noise in addition to variations in the sky background.

Before the advent of nod & shuffle, it was basically impossible to obtain a deep [S III] 9069,9532 or [O I] 6300 observation of a galactic source. This is unfortunate because the former is an important pressure diagnostic, and the latter is prominent in partially ionized and/or shocked regions.

There is also a “straddle” mode to nod & shuffle imaging. If we are observing a field set against a slowly varying sky (e.g., moonlight, Gegenschein, cirrus), the off-fields can be taken from either side of the target field (cf. Section 3.4).

3.6. *Time series imaging*

For time-varying sources, we can step the charge in one direction while switching between a line and a reference frequency. For example, a compact variable source imaged through a narrow aperture in the focal plane forms a narrow image at the detector. We can switch between the line and a reference frequency many times forming a set of narrow interleaved images at the detector. The reference frequency is a measure of the atmospheric stability during the time series. Alternatively, if nearby reference stars are available for photometric calibration, then charge shuffling can be done at a single fixed frequency.

By way of example, some X-ray binary stars (see Section 11 below) produce strong emission lines that vary on 0.1 Hz timescales. Using the TTF, with a slit only 4 pixels wide, we can obtain 500 images in the emission line, interleaved with a further 500 images at a reference frequency. In this example, all of the CCD area is utilized because the charge is clocked in only one direction. The vertical shift takes about 50 μs per row. Strictly speaking, this operation constitutes a charge "shift" rather than a charge "shuffle". Once the chip is full, it takes $\sim$3 min to read out the CCD.

If the read-out time of several minutes is critical to the measurement, an alternative method is time series read-out. For the example above, the four CCD rows comprising the slit are clocked downwards at the end of each exposure. However, the next exposure is delayed by the time it takes to read out the bottom four rows ($\sim$200 ms). In practice, the slow shutter means that the time series mode is to be preferred for most applications over the 'charge shift' mode.

3.7. *Unidirectional charge stepping with a focal-plane slit*

As strange as it may appear, there are times when we need to produce a long-slit spectrum with a tunable filter. We simply illuminate OSIRIS with a monochromatic source in the presence of a focal-plane slit, and then step the plates through all possible settings while clocking the charge down the CCD. While this is vastly less efficient than using a long-slit spectrograph, the capability is a fundamental component of establishing the parallelism of reflecting mirrors at few micron spacings (Jones & Bland-Hawthorn 1998).

We do this by taking long-slit TTF spectra of an arc line, with a pupil-plane mask to isolate one quadrant of the tunable filter. This operation is repeated for each quadrant. The plates are adjusted until the line shows peak transmission at a common plate setting for all four quadrants of the beam. It is then that the plates are parallel. Using this technique, we are also able to observe phase reflectance effects at very narrow gap spacings. Conventional methods of aligning plates are an order of magnitude slower by comparison.

3.8. *Other modes*

With a versatile instrument like OSIRIS, there is the potential for other observing modes not planned for at present. To give one example, at the AAT, we have experimented with forced drift scanning where the telescope is trailed in declination in synchrony with the charge on the chip being clocked vertically. This attempts to simulate drift scanning although the results are a poor cousin to the real thing. Only about half of the available field of view can make use of this method.

4. DIFFERENTIAL SCIENCE

So now that we have access to a truly differential imaging spectrometer, what are the science areas which are likely to benefit? Consider the table below. OSIRIS will allow the observer to combine charge shuffling with switching between any combination of a narrow, intermediate, or broad band.

For example, the OSIRIS filter wheel will allow rapid movement between two broad band filters, say u' and z', in order to obtain an accurate $u' - z'$ color for every pixel of a galaxy image. Abrahamet al. (1999) show the power of this type of work, even at the redshifts of the Hubble Deep Field. In this particular example, OSIRIS will be relying on the flatness of the detector to assist in the sky subtraction. The Sloan Survey uses drift-scanning which results in superb pixel–pixel flatness over the detector. Of course, the Sloan survey is restricted to Gunn filter bands on a small telescope; OSIRIS observations will get down to much fainter levels.

A particularly rich area for OSIRIS will be differential measurements based on emission line and absorption line indices. When we observe astronomical sources at a given wavelength, they often look very complicated. This has led to a widespread impression that observing galaxies at too close a range subjects you to "weather" rather than important physical insight. But the complexity often arises from beating between various physical parameters. This point was well made in Peimbert's talk on abundance gradients in spiral galaxies (Peimbert & Peimbert, this volume, p. 117). The abundance trends are often very noisy *until* one takes into account temperature effects, whereupon the trends become clear.

If a diagnostic pair of lines can be chosen which, when ratioed, reveal a single physical dependence, the resulting map can look much more organized than the individual images taken separately. A striking demonstration of this is shown in figure 4 of Shopbell & Bland-Hawthorn (1998) in their study of the galactic wind in M82. The [N II]/Hα map reveals narrow bipolar cones in accord with the gas kinematics. The radiation from the hot young stars in the disk escapes along the cones and photoionizes the compressed gas, thereby lowering the temperature of the gas compared to shocked material further out. This is what is seen in the ratio map.

Emission line diagnostics are well suited to tunable filters since the spectral lines should be closely spaced in wavelength, as first pointed out by Baldwin, Phillips, & Terlevich (1981, hereafter BPT; the reader is encouraged to look at the Ten Commandments of spectroscopic diagnostics in Veilleux

TABLE 1

DIFFERENTIAL OBSERVING MODES

			1st band	
		Narrow	Intermediate	Broad
	Narrow	BPT-VO-KD	Strömgren	Straddle
2nd band	Intermediate	Strömgren	Lick index	Stromgren
	Broad	Straddle	Stromgren	$u'g'r'i'z'$ color

2002a). The OSIRIS blocking filters, which isolate an order of interference, inflict that on you in any case. Indeed, the chosen OSIRIS bands pay heed to the important diagnostics discussed by BPT, Veilleux & Osterbrock (1987, hereafter VO), and Kewley et al. (2001, hereafter KD). It will enable us to obtain very accurate diagnostic maps (of temperature, ionization, density, abundance) in standard ratio pairs across the optical spectrum.

For the record, it is worth noting two things about the use of tunable filters with OSIRIS. Like TTF, OSIRIS covers the optical range in two bands which purposefully overlap at Hα. This is much the most important emission line comparison in the optical range and it can be reached within both the blue and red TF. Furthermore, while the option has not been proposed for OSIRIS, differential imaging can be obtained between two very widely spaced spectral bands with the aid of a multiband filter (Cianciet al. 2000; Offer & Bland-Hawthorn 1998). This has been used to great effect in Cianci's (2002) thesis work to derive accurate dust maps by comparing Hα and Hβ pixel by pixel across the full field of nearby spiral galaxies.

The use of broad band photometry coupled with stellar population synthesis is a well-established technique for probing the star formation history of galaxy populations from integrated starlight. The power of the method is its simplicity although it cannot uniquely disentangle the age–metallicity degeneracy (Bicaet al. 1990). Another widely used technique is the Lick index system (Bursteinet al. 1984) refined by Worthey and Trager. OSIRIS will allow for differential imaging with both methods. Vazdekis (1999) has shown the importance of spectral diagnostics with a fourfold increase in resolution over the Lick indices. There is now an active area of research across the Spanish and Mexican communities to identify sensitive population diagnostics accessible to tunable filters.

5. TAURUS TUNABLE FILTER—THE FIRST FIVE YEARS

We now provide a short review of the first five years of observing with the Taurus Tunable Filter at the AAT; for the first three years, the TTF was also used at the WHT. The instrument has had most of its use on the AAT, where it gets between 10–15% of the telescope time scheduled by the PATT (UK) and ATAC (Australia) committees. In a nutshell, the TTF allows for wide field (10′) spectrophotometric imaging from 370 nm to 1000 nm with resolving powers generally in the range 100 to 1000. An important feature of the instrument is the use of charge shuffling synchronized to band switching in order to greatly suppress systematic errors associated with conventional imaging. Another aspect of the TTF is time series read-out coupled to band switching which has led to important new work on compact variable sources. Technical accounts of the instrument, and its related charge shuffling modes, can be found in the Appendix and on the TTF web site `www.aao.gov.au/ttf`.

There have been several independent reviews on tunable filters including Bessell (2001), Jones (2001a), and Jones et al. (2001). Recent scientific reviews can be found in Veilleux et al. (2002) and Veilleux (2002b,c). A long list of largely unexplored science areas with tunable filters is given in Bland-Hawthorn et al. (2001).

The purpose of this review is to stress the versatility of tunable filters in observational astronomy. The Taurus-2 focal reducer has also produced important results in its other modes of operation: polarimetry, Fabry–Perot "staring" and emission line scanning, and most recently multiobject spectroscopy (see www.aao.gov.au/taurus for more details). But here we concentrate specifically on the TTF mode of operation.

All observations discussed here were undertaken on 4 m telescopes, often in non-ideal observing conditions. This author eagerly anticipates the tunable filters which are planned or under way for the

Science with the GTC 10-m Telescope (Granada, España, 5-8 febrero 2002)
Editors: José Miguel Rodríguez Espinosa, Francisco Garzón López & Verónica Melo Martín

new generation optical/IR telescopes on superb sites. These include, inter alia, the OSIRIS tunable filter on the 10 m GTC (Cepa et al. 2002), a possible tunable filter within FORS on the VLT, the proposed Maryland Magellan tunable filter (MMTF), and the tunable filter within the Goodman spectrograph on the SOAR 4 m telescope. When one reviews the results below, it is important to keep in mind that the new generation of tunable filters need only improve on one of the following—site conditions, instrument performance, field of view, pixel sampling, telescope aperture—to achieve a major gain. The proposed or planned instruments are expected to make major gains on at least three out of five!

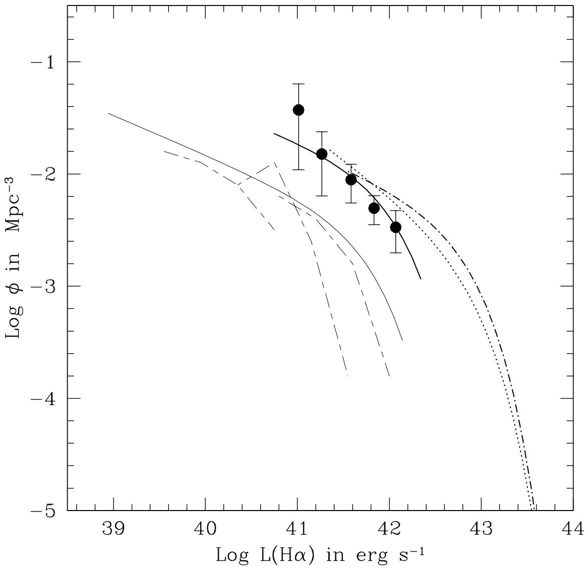

Fig. 1. The evolution of the Hα luminosity function with redshift, taken from Tresse et al. (2002, figure 13). The filled circles are the data points from their ISAAC/VLT survey. The short–long dashed curves are the preliminary Hα LF from Jones & Bland-Hawthorn (2001) from left to right respectively at $z = 0.08$, $z = 0.24$, $z = 0.40$. The other curves are defined in Tresse et al. (2002).

6. SURVEYS OF STAR FORMING GALAXIES

6.1. *Field*

In so many ways, tunable filters are ideally suited to surveys of star forming galaxies in different environments. The object selection is based on the property we are trying to measure, i.e., the star formation rate via the Hα line. This was the principle behind the TTF Field Galaxy Survey which was the basis of D. H. Jones's thesis (2001b). He obtained photometric Hα data and restricted Hβ data on clfour usters and nine field positions. All observations were highly successful in identifying line emitting galaxies, typically 10–40 objects above 3σ per pointing (although rather fewer in Hβ), finding many more objects than comparable studies with conventional imaging techniques (e.g., Hu & McMahon 1986; Thommeset al. 1998). The first part of TTF Field Galaxy Survey was published in Jones & Bland-Hawthorn (2001).

Recent evidence suggests a decline in the volume-averaged star formation rate (SFR) with the advance of cosmic time since $z \sim 1$. The survey set out to derive Hα luminosity functions in three discrete wavelength intervals at $z = 0.08$, 0.24, and 0.39. One of the interesting surprises was a population of compact sources found to have moderate amounts of Hα emission: some of these sources would have been dismissed as stars in earlier photographically selected surveys.

In a new study of galaxies in the Canada–France Redshift Survey (CFRS), Tresseet al. (2001) combine the TTF Field Galaxy Survey measurements with their ISAAC/VLT Hα luminosity function at $z \sim 1$ (see Figure 1). They find that the comoving Hα luminosity density increases by a factor of 12 from $z = 0.2$ to $z = 1.3$. Their results confirm a strong rise of the star formation rate at $z < 1.3$ proportional to $(1 + z)^{4.1\pm0.3}$.

Glazebrook (1997) has used the TTF to study star formation in the Hubble Deep Field North. In collaboration with R. Abraham, he sampled almost 70 narrow band images in four redshift intervals. In this way, one gets a *multiplicity effect* in that the same images can be used to find different sources at different redshifts, thereby allowing for a derivation of the star formation rate over a wide range in redshift. The data, which were taken during four long dark nights at the WHT, have superb photometric quality (point spread function over 70 summed images $\approx 0.7''$); the analysis is not yet complete.

6.2. *Clusters*

Until now, identifying most cluster members from a combination of kinematics and a color–magnitude diagram has been difficult, particularly for blue objects, because of contamination of sight line galaxies. But TTF observations can be used to identify faint cluster members unambiguously, in particular those with line emission. These objects are typically blue, so the TTF is an ideally suited to unscrambling the region of contamination (see Figure 2b). We find that k + a galaxies (Dressler & Gunn 1983) can also be identified from Hα absorption (Jones & Bland-Hawthorn 1999, figure 1).

Science with the GTC 10-m Telescope (Granada, España, 5-8 febrero 2002)
Editors: José Miguel Rodríguez Espinosa, Francisco Garzón López & Verónica Melo Martín

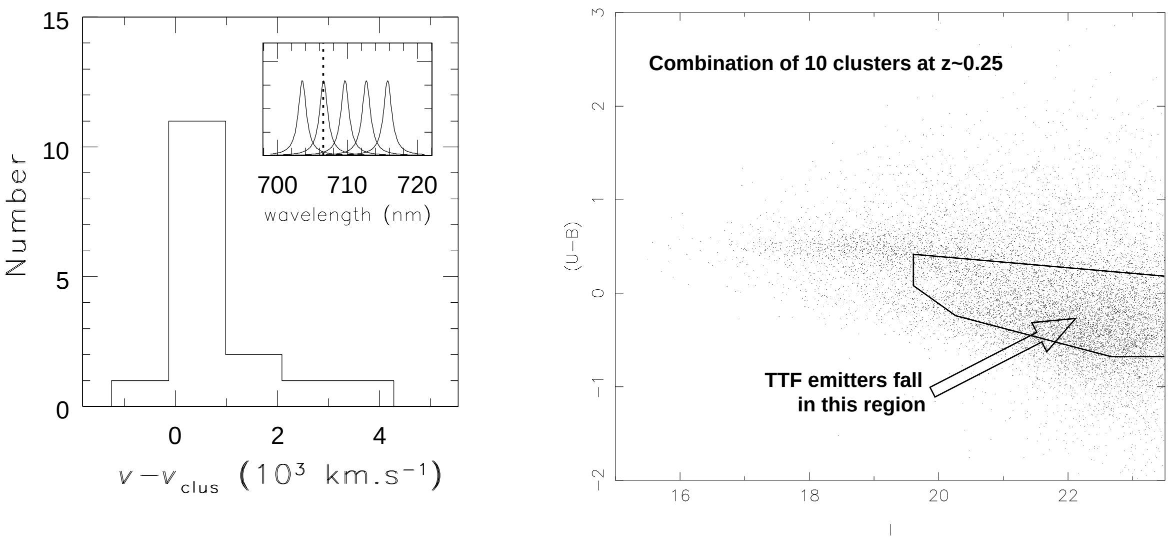

Fig. 2. Left: Distribution of emission line objects from a $z = 0.4$ cluster field if all of the emission is assumed to be redshifted Hβ. The inset shows the TTF passbands relative to the wavelength of redshifted Hβ (dotted line). Right: Illustration of where the line emitters fall in a cluster color–magnitude diagram. The cluster data are from Smail et al. (1998).

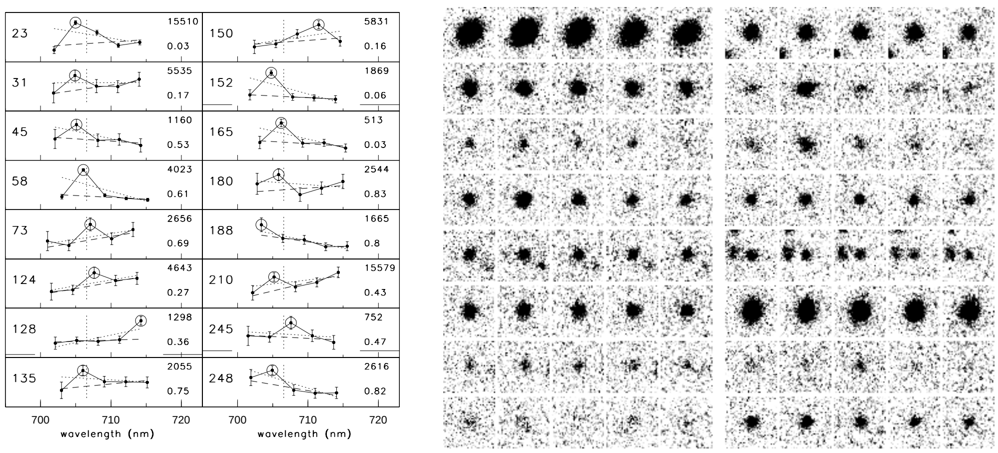

Fig. 3. TTF spectra (left) and scans (right) for a sample of emission line cluster candidates. The number on the left of each panel is the object ID, the numbers at right are the flux in counts (top) and shape classification parameter (bottom; 1 = stellar, 0 = galaxian). No attempt has been made to reject possible fore/background contaminants on the basis of appearance or redshift. The vertical dotted line denotes the cluster redshift from Keck spectra of ∼10 galaxies in the field. The wavelength shift of spectra between objects is due to the off-axis phase effect across the TTF field (Bland-Hawthorn & Jones 1998a).

In Figure 3, we demonstrate the power of TTF to find line emitters even in poor seeing ($2''$). Dalcanton (1996) and Zaritsky et al. (1997) use CCD drift-scanned images to identify clusters through enhanced surface brightness fluctuations out to $z \approx 1.1$. For one cluster at $z = 0.45$, in just two hours, we identified ten cluster members at the AAT in $2''$ seeing, compared to six members in 1.5 nights using the Keck LRIS spectrograph.

For the rich cluster A3665 (AC 106), first studied by Couch & Newell (1984), Zaritsky & Jones identify 40 Hα emitting candidates above 3σ, with many more candidates at lower thresholds (down to 0.03 solar masses per year at $z = 0.25$), in just four hours. Example TTF scans are shown in Figure 3b, with the Hα line profiles in Figure 3a.

To date, average star formation rates in $z = 0.2$–0.5 clusters appear to be quite low compared to the field (cf. Couch et al. 2001).

6.3. *Quasar environment*

Bakeret al. (2001) used the [O II] 372.7nm line to detect starforming galaxies in the vicinity of MRC B0450-221. Many emission line galaxies were easily identifiable by eye over the whole field (down to a few solar masses per year). Their projected separations from the quasar range from 200 to 700 kpc. A nice demonstration of the power of TTF imaging is the detection of very faint extended [O II] emission along the radio axis of the quasar.

6.4. *Quasar sight lines*

Francis, Wilson, & Woodgate (2001) and Francis et al. (2001) have continued their study of the "Francis cluster", an extended ensemble of galaxies at $z = 2.38$ that was originally identified from the damped Lyα absorption occurring at the same redshift in a paired quasar sight line. In this study, they look for Lyα emission from star forming galaxies within the ensemble. It is clear that the future holds great promise for using quasars to identify gas-rich star forming environments at high redshift.

7. ENERGETIC GAS IN CLUSTERS

There have been claims of EUV excesses in clusters which, if true, would suggest that 10^{5-6} K gas accounts for a large fraction of missing baryons (Lieu et al. 1999; Bowyer, Berghöher, & Korpeler 1999). EUV emission is exceedingly difficult to detect at Earth: it is too hot to be detected optically, too cool to be seen by X-ray satellites, and undergoes molecular line absorption as it propagates through the ISM.

Using the *EUVE* satellite, Lieu et al. (1999) claim a direct EUV detection of the cluster Abell 1795. Maloney & Bland-Hawthorn (2001) found that such a strong EUV field would ionize the molecular and H I disks of all spirals in the cluster to such an extent that they should all be Hα bright. TTF observations of the cluster were kindly taken by A. Edge in "straddle shuffle" mode in order to subtract the continuum light of the cluster very accurately. Only very faint Hα emission was found in the cluster spirals.

Jaffe & Bremer (2000) used "on–off" charge shuffling in order to detect very faint levels of Hα emission in cooling flow clusters. In the case of Abell 2597, they find a nebula extending over 50–60 kpc from the cluster centre. A. Edge and collaborators have looked at a large sample of cooling flow clusters and detect optical line emission in all cases. R. Johnstone and collaborators have begun a campaign to detect very highly ionized gas from ions like [Fe X].

8. GRAVITATION LENSING

Tunable filters are ideal for extended sources, in particular, irregularly shaped sources with no axis of symmetry. Earlier work with D. H. Jones on star formation in clusters occasionally turned up spectacular gravitational lenses throughout the cluster. As seen through the TTF, these sources can have high contrast because the background object is commonly a high redshift star forming galaxy which emits strongly in emission lines. Hewett et al. (2000) used the TTF to look for extended emission in a galaxy–galaxy gravitational lens due to an intermediate redshift elliptical lensing a $z = 3.59$ star forming galaxy. They were following up a suggestion by Miralde-Escudè & Lehar (1992) that the surface density of high redshift star forming galaxies is so high, galaxy–galaxy lensing should be relatively common.

9. GALAXIES

The tunable filter has the major advantage of providing detailed spectrophotometric information over a larger field of view (FOV) than that of other 3D instruments. It would be very difficult and very expensive to build an integral field spectrograph that could provide the same field and the same photometric integrity at low light levels. The tunable filter is therefore ideally suited to study nearby galaxies where the line-emitting gas extends over several arc minutes. This ionized material is an excellent probe of the phenomena taking place in the core of starburst and active galaxies and can be used to quantify the impact of nuclear and star formation activity on the environment and vice versa. Once again, the reader is encouraged to look at recent reviews by Veilleux (2002b,c).

9.1. *Radio galaxies*

Tadhunter and collaborators have undertaken a comprehensive survey of extended ionized haloes of powerful radio galaxies (Tadhunter et al. 2000; Solorzano-Inarrea et al. 2002). It is well known that optical line emission often aligns with the radio axis, as these authors find in all cases. But what was more surprising was the frequency of optical emission perpendicular to the radio axis. In Figure 4, the optical emission in Coma A extends over more than 150 kpc in an egg-shaped nebula (Tadhunter et al. 2000). More remarkably, the faint outer nebula emission matches the extended outer radio lobe over these same scales.

The frequent match-up between optical, radio, and X-ray emission in radio, Seyfert, and starburst galaxies is a topic of great interest (see below). But this cannot be uniformly ascribed to shocks. In the case of low power radio jets, the emission is thought to arise from synchrotron, whereas in high power radio jets, the X-rays appear to arise from inverse Compton emission (Birkinshaw, Worrall, & Hardcastle 2001)

9.2. *Quasar nebulae*

Shopbell et al. (1999) recently announced a remarkable extended nebula surrounding the X-ray selected quasar, MR 2251-178. The summed image in Figure 5 is one of the faintest extended emission line images ever published. The nebula, which extends over more than 200 kpc, shows pronounced tidal arm structure. These authors chose two narrow bands spaced by half a bandwidth in order to study the kinematics. The entire structure appears

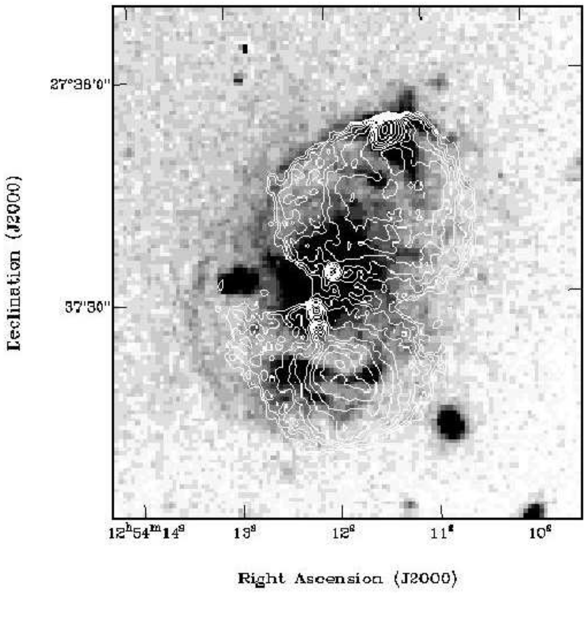

Fig. 4. Deep TTF image of Coma A in Hα from Tadhunter et al. (2000). A complex spiral nebula is seen to extend over 150 kpc. The overlaid radio continuum map (contours) shows striking similarities to the distribution of ionized gas.

to be in rotation about the quasar. The gas is not obviously connected with any other companions in the field. UV radiation from the quasar would have to be escaping almost isotropically to account for the ionization. Both the source of the gas and the source of ionization remain a mystery.

9.3. *Seyfert galaxies*

Seyfert galaxies have long held a particular fascination for the present author. Here we so often see the impact of the nuclear activity on the very large scale disk of a spatially resolved galaxy in the near field. Two of the most recent and spectacular examples are NGC 1068 and NGC 7213. Can we use the ISM as a screen to interpret what is essentially unresolved and unseen at the core?

NGC 1068 is one of the most remarkable of Seyfert galaxies in the near field; it is well known that the core harbors a concealed Seyfert 1 ("low power quasar") nucleus, but just how energetic is the source? The radio jet axis exhibits a wide range of activity (Cecil et al. 2002) but can we infer the true energetics and nuclear spectrum from multiwavelength studies (Alexander et al. 2000; Pier & Krolik 1993)?

Shopbell et al. (2001; see also Veilleux 2002a) find that the well-known ionization cone (Pogge 1988) extends up to and *beyond* the H I edge of the early-type spiral. The observed nebula requires rather special conditions to be easily seen over so many scale orders. The most likely interpretation is that a multiphase, vertically distended ISM is being blasted by a very energetic central source ($L_{uvx} > 5 \times 10^{43}$ erg s^{-1}). Indeed, the *Chandra* observations appear to show the most spectacular example to date of an "X-ray ionization cone" (Young, Wilson, & Shopbell 2001).

Such galaxy-scale ionization cones are not unique to NGC 1068. Another has been detected with the TTF in NGC 7213 (Rupke et al. , in preparation; Veilleux et al. 2002) to rival the spectacular system in NGC 5252 studied by Tadhunter & Tsvetanov (1989). Ionization cones are often associated with nuclear jets. Recent examples from TTF observations include IC 5063 (Cecil et al. 2001) and Circinus (Veilleux & Bland-Hawthorn 1997). Circinus, a large spiral close to the Galactic plane, is particularly noteworthy: the system shows evidence for a whole network of "artillery shells" blasting away from the nucleus. One such filament shows a spectacular "Herbig–Haro"-like morphology.

Extended ionization cones are seen in a variety of sources, including the radio galaxies studied by

Science with the GTC 10-m Telescope (Granada, España, 5-8 febrero 2002)
Editors: José Miguel Rodríguez Espinosa, Francisco Garzón López & Verónica Melo Martín

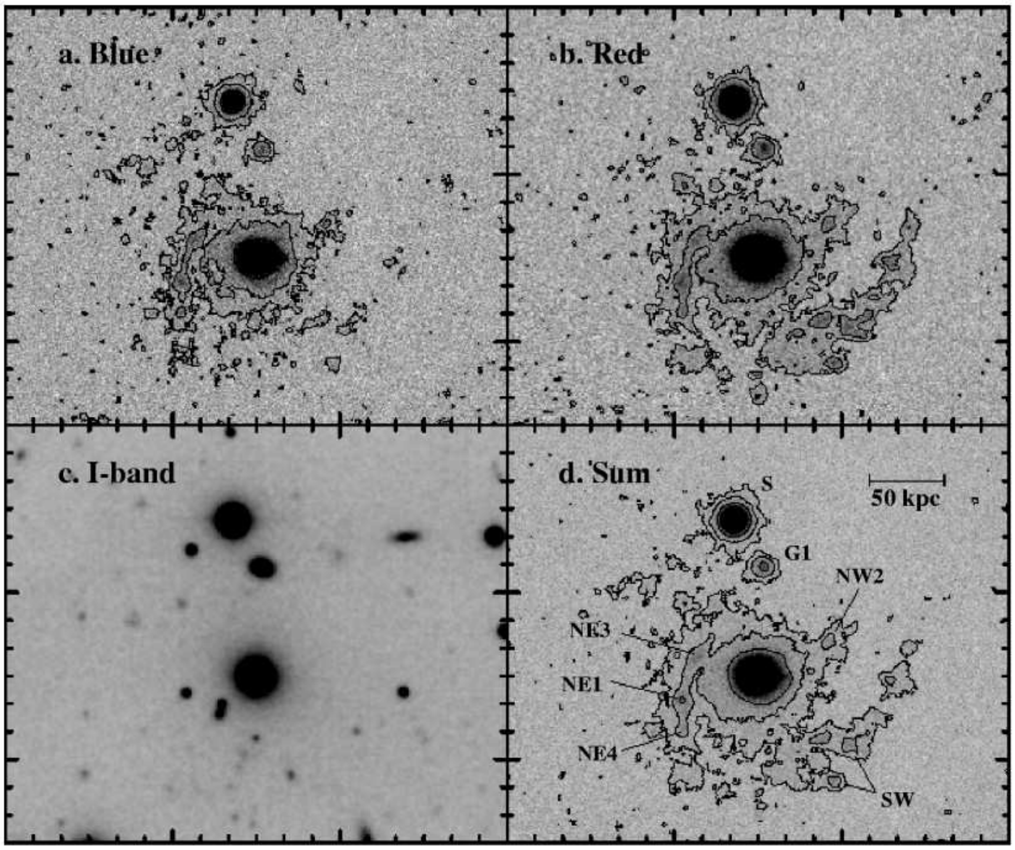

Fig. 5. The extended ionized nebula surrounding the X-ray-selected quasar MR 2251-178. The top figures show deep TTF Hα images in two closely spaced narrow bands in order to emphasize the kinematic structure. The summed emission (bottom right) is seen to extend over 200 kpc or more. The stellar continuum image is also shown (bottom left).

Tadhunter (see above). This author has obtained a short exposure [O III] image of Cen A using the straddle shuffle mode in order to achieve a clean subtraction of the elliptical galaxy. In Figure 6, we find a very highly ionized halo of [O III] emission above and below the dust lane. The component was first discovered by Phillips et al. (1984), who found that the faint emission appeared to rotate slowly compared to the dust lane, and typical line dispersions are hundreds of km s^{-1} FWHM. We suspect that this emission arises from a highly ionized wind that encompasses the radio jet over a much larger solid angle.

Cecil et al. (2000) show that the famous braided jets in NGC 4258, which can be traced over 10 kpc or more, emanate from the nuclear regions. These jets have been seen in radio continuum, *ROSAT*/*Chandra* X-rays, and optical emission. They obtained deep Hα observations in the outer H I disk and discovered faint tendrils of the jets far beyond what was known before. A re-analysis of the radio continuum data has revealed that these faint features have radio counterparts.

The beautiful NGC 1068 and NGC 4258 observations show faint emission which extends far beyond what was previously known. It is important to realize that both observations were taken in full moon. The TTF is a highly effective *bright time* instrument.

9.4. *Starburst galaxies*

A number of powerful starburst galaxies show evidence for large scale winds along their minor axis (see reviews by Veilleux et al. 2002 and Heckman 2002). This phenomenon appears to be common at low and high redshift (Lehnert & Heckman 1996; Veilleux et al. 2002; Pettini et al. 2001). The most detailed studies have concentrated on objects like M82, NGC 253, and NGC 3079. It remains unclear just how much energy, mass and metals these objects contribute to the intergalactic medium (IGM).

Science with the GTC 10-m Telescope (Granada, España, 5-8 febrero 2002)
Editors: José Miguel Rodríguez Espinosa, Francisco Garzón López & Verónica Melo Martín

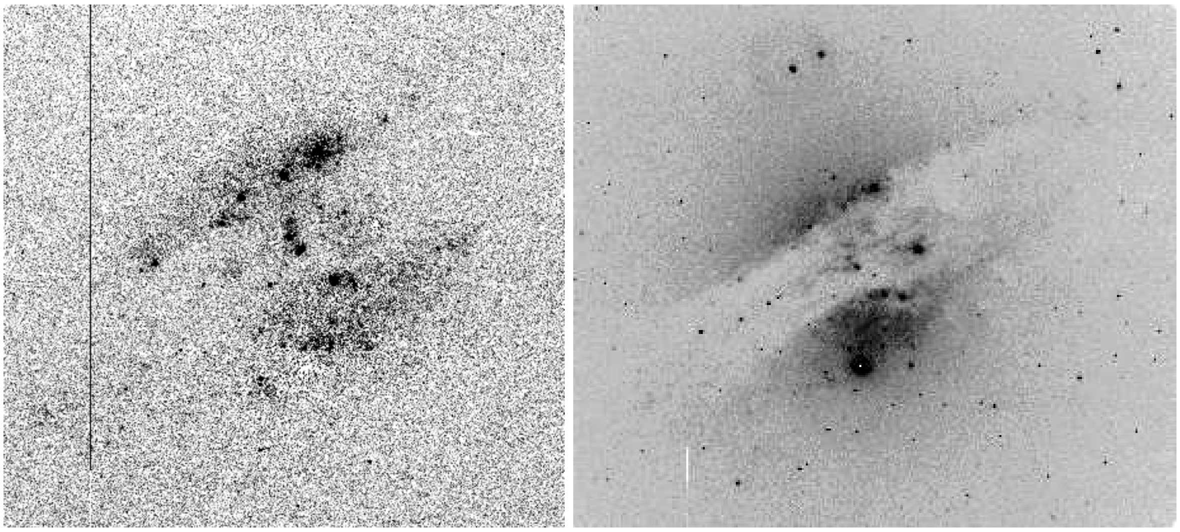

Fig. 6. Left: Short exposure [O III] 500.7 nm emission line halo seen above and below the dust lane in Cen A, obtained with the "straddle shuffle" mode using the TTF (see text). These are raw data: the bad column arises from trapped charge during the charge shuffling. Right: Line + continuum image of Cen A in order to emphasize the dust lane.

In some cases, it is not clear if the wind is driven by a central starburst, an AGN, or a combination of these. But there is mounting evidence that the optical diagnostics may greatly underestimate the true wind energetics (Strickland & Stevens 2000).

Veilleux & Rupke (2002) provide spectacular evidence for a large scale wind in the edge-on, early type galaxy NGC 1482. They obtain a clear separation of disk material from the outflowing gas. The kinematics show all the hallmarks of a biconal outflow. More impressively, the entire emission line complex has diagnostics which are entirely consistent with fast shocks. In other wind systems, there is often a large contribution from the central ionizing stellar radiation field.

Science with the GTC 10-m Telescope (Granada, España, 5-8 febrero 2002)
Editors: José Miguel Rodríguez Espinosa, Francisco Garzón López & Verónica Melo Martín

9.5. *Disk–halo connection in spirals*

For his thesis work, Miller (2002) is undertaking an emission line survey of edge-on spiral galaxies in order to trace the connection of disk star formation with activity in galactic haloes. Miller & Veilleux (1999) and Veilleux (2001) show spectacular examples of diffuse ionized gas several kiloparsecs off the plane of normal spirals. The ratio maps show enhanced [N II] emission with respect to Hα as we move away from the plane which is most easily explained as a higher electron temperature in the halo gas (cf. Sokolowski 1993; Reynolds, Haffner, & Tufte 1999; Collins & Rand 2001). The source of the temperature increase is a topic of debate in contemporary astrophysics.

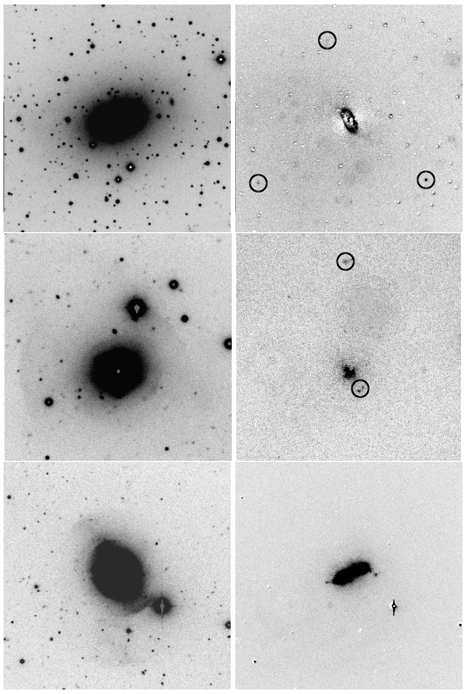

Fig. 7. R band continuum images of elliptical/S0 galaxies (left) and their associated Hα emission line images (right) from the TTF survey of Ferguson et al. (2001).

9.6. *Star formation in elliptical and spiral galaxies*

Very little is known about the frequency and nature of star formation in the earliest types of galaxies, even though we have known for a long time that a large fraction contain cold gas (van Gorkom 1997; Knapp 1999). Ferguson and collaborators (2001) have been making Hα observations with TTF of a large sample of H I-selected ellipticals. Essentially all of these systems (see Figure 7) show evidence of star formation to date.

For her thesis work, Cianci (2002) is undertaking a detailed comparison of face-on spirals observed at Hα and Hβ, and UV images from the Ultraviolet Imaging Telescope (see Figure 8). Her particular interest is to understand the connection of the diffuse ionized gas with the H II regions and dust distribution (cf. Zurita 2001; Zurita et al. 2000). Spiral arms are sometimes quite asymmetric with respect to each other in their detailed properties. In one galaxy, M83, she finds a large complex which has an enhanced UV continuum and relatively faint Hα emission (Cianci 2000). This stellar association may be a relic of a recent star forming complex which appears to have survived several disk rotations.

NGC 2915 is a dark matter dominated, blue compact dwarf galaxy with an H I disk extending to a radius of 15 kpc. In optical continuum, it is a relatively nondescript with an optical radius of only 3 kpc. No stars were known to exist beyond this radius. Meurer et al. (1999) obtained deep Hα imaging with the TTF, revealing, for the first time, faint H II regions at projected radii of 3 to 6 kpc.

Higdon et al. (1997) have undertaken a multiline study of the Cartwheel Galaxy. This is the most spectacular of the class of "ring galaxies" which are excited by the central impact of an interloper. They identify up to 100 star forming regions throughout the disk, which they will model as propagating star formation. There is a related class of galaxies excited by off-center impacts. One of these, NGC 1512, has been looked at in detail with the TTF by F. Briggs. Moreover, there is a wider class of objects under the general heading "event-driven star formation" (strong mergers, jet induced star formation, etc.) which are relatively unexplored with the TTF.

9.7. *Stellar populations in galaxies*

One of the most important areas where very little work has been done is imaging in stellar absorption lines. Beauchamp & Hardy (1997) have demonstrated that this is possible even with small aperture telescopes. Molla, Hardy, & Beauchamp (1999) emphasize the importance of spatially resolved, stellar absorption line mapping of face-on spiral galaxies. S. Ryder and colleagues have begun to look at the potential of TTF for this sort of work. They choose TTF bands that mimic Lick indices, and calibrate the system performance with observations of Lick index standards. Bland-Hawthorn et al. (2001) provide a list of stellar absorption line projects which should be considered for tunable filter work.

10. GALACTIC SOURCES

10.1. *Pulsar wind nebulae*

Jones et al. (2002a) found an extended Hα nebula associated with a pulsar moving rapidly through the interstellar medium. Several of these sources are now known, but in the case of pulsar B0740-28, the conic nebula is pinched perpendicular to the long axis. Possible interpretations are variations in the pulsar wind or in the external ISM.

10.2. *Interstellar medium*

Schuberth & Burton (2000) used the TTF to observe arguably the most exotic line to date in the optical, the [C I] 872.7 nm line buried deep within the OH forest. This line is extremely important in photodissociation regions (PDRs). NGC 2023 is an H II region on the surface of a molecular cloud. These authors postulated that carbon atoms emitting at 872.7 nm might delineate the PDR. Their [C I] image (see Figure 9) is the first true image of extended carbon emission ever obtained. They show that the emission correlates very closely to the so-called mysterious extremely red emission (ERE) at about 650 nm. [C I] is clearly a powerful tool for probing galactic star forming regions.

10.3. *Weather in brown dwarfs*

There is presently a lot of interest in detecting variability from brown dwarfs. If the atmospheres and environs are cool enough, models suggest that there should be dust condensations swirling around the brown dwarf producing variability in the light curve. This was detected for the first time by Tinney & Tolley (1999) in the M-type brown dwarf LP 944-20. They used TTF in a novel set up which required the charge to step on the CCD in synchrony with the TTF being tuned between different bands. Since then, variability has been found in another brown dwarf Kelu-1 by Clarke, Tinney, & Covey (2002). These sources do indeed appear to have complex weather patterns.

10.4. *Variable stars*

Deutsch et al. (1998) have used TTF in time series mode to study the [O I] 844.6 nm emission line from the X-ray binary star V2116 Oph, the optical counterpart of GC1+4. The symbiotic-like optical spectrum of V2116 Oph shows the presence of a red

Science with the GTC 10-m Telescope (Granada, España, 5-8 febrero 2002)
Editors: José Miguel Rodríguez Espinosa, Francisco Garzón López & Verónica Melo Martín

Science with the GTC 10-m Telescope (Granada, España, 5-8 febrero 2002)
Editors: José Miguel Rodríguez Espinosa, Francisco Garzón López & Verónica Melo Martín

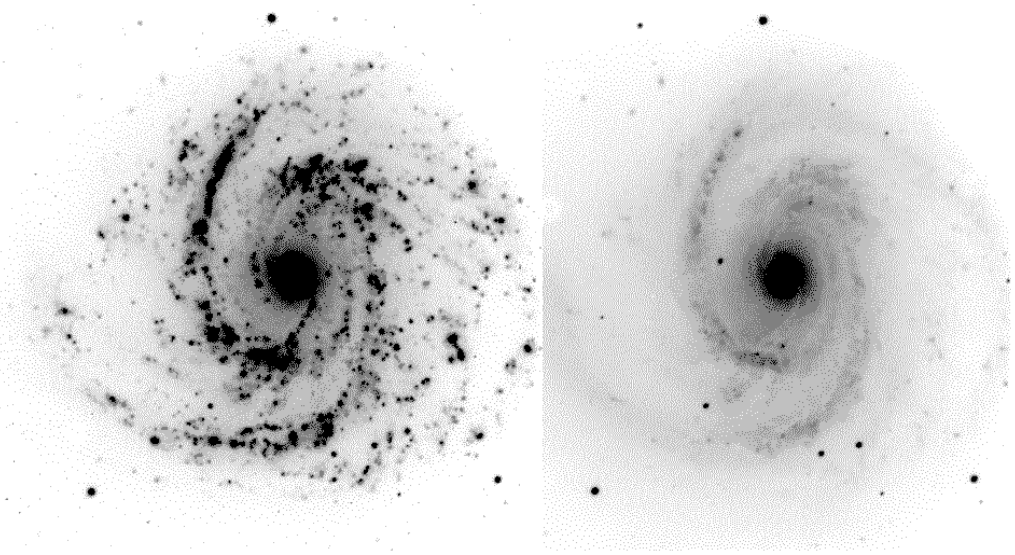

Fig. 8. A demonstration of the superb contrast possible when observing a face-on spiral through a narrow band tuned to Hα (left) compared to a neighboring continuum band (right). Both images were taken with the TTF and come from Cianci's (2002) spiral galaxy survey.

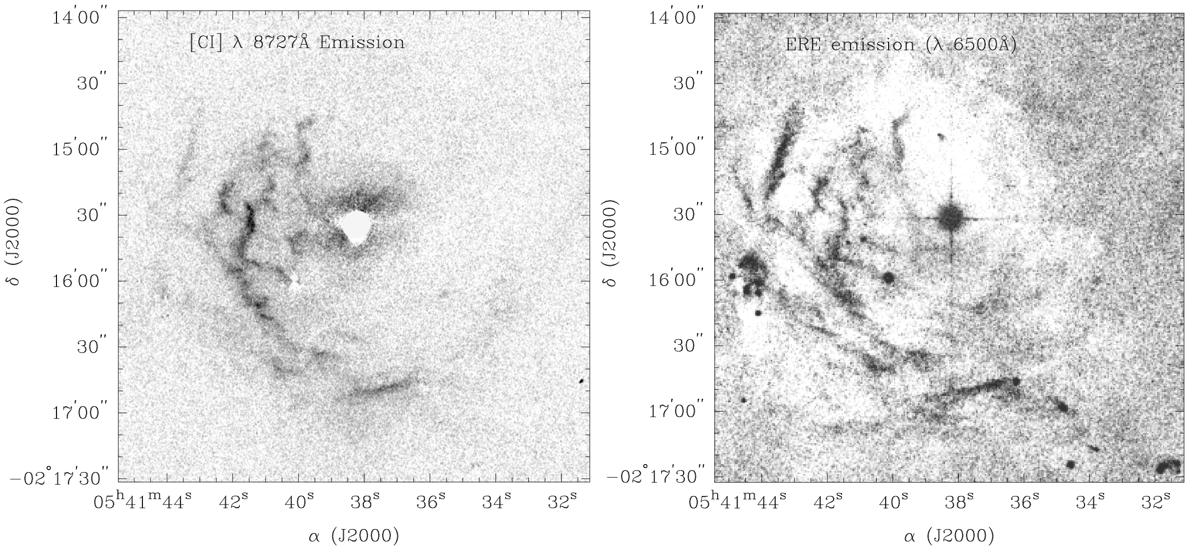

Fig. 9. Schuberth & Burton (2000) note that the left image is the first true map of carbon emission ever obtained. It was made possible by the TTF observing in an ultranarrow band set to transmit the [C I] 872.7 nm emission line. Note the remarkable similarity with the extremely red emission (ERE) shown on the right, although the ERE emission is generally brighter further away.

giant. The X-ray source is highly variable, so the [O I] line was studied in the hope of detecting variability. This was rejected to a high level of confidence. It is thought that the system is being seen at a special time, and is probably an X-ray pulsar undergoing rapid evolution.

10.5. *Planets*

Ryder (2001) was able to image Mars in four narrow bands, a difficult experiment since the source is so bright. With four bands set at 390, 500, 668, and 707nm, he produced superb images of the ice caps, albedo features, and various cloud formations.

11. ISSUES

There are numerous ways in which tunable filters can find new and important uses in astronomical programs. One possible advance for tunable filters are devices which can operate at cryogenic temperatures. Problems like piezo creep and slow gain at cryo temperatures can now be overcome.

The largest tunable filter that Queensgate can make (150 mm aperture) is not well suited to 8–10 m telescopes. But there is no reason why a 300 mm aperture etalon, for example, cannot be made. We have an initial design for such a system that uses an additional control stack at the center of the plates, well matched to the central obstruction of most telescopes. This design requires a slightly reconfigured CS100 control system.

It is commonly thought that tunable filters are restricted to switching between bands which fall within the restricted bandpass of the order sorting filter. In fact, a multiband order sorter (Offer & Bland-Hawthorn 1998) allows spectral bands at opposite ends of the optical spectrum to be observed in sequence (Cianci et al. 2000).

There exists a wide class of sources which have never benefited from detailed narrow band imaging largely because even through conventional narrow bands, the field stars saturate the detector. One of many examples was an attempt to measure gas metallicities in the vicinity of the Trapezium. However, rapid switching through differential ultranarrow bands makes this entirely feasible now. The straddle shuffle demonstration by Maloney & Bland-Hawthorn (2001) has been used on galaxies with very bright disks and cores, leading to perfect cancellation of the continuum light and therefore revealing very weak levels of line emission. This same method should work well on young globular clusters in order to search for Hα emission, but this has not been attempted to date.

Tunable filters have major applications for adaptive optics imaging and for coronographic imaging. The use of differential narrow band imaging would greatly help to suppress any stray light around the central or nearby bright stars. B. Woodgate has achieved some spectacular observations of emission line nebulae around symbiotic stars with the *Hubble Space Telescope*, but the central stars are so bright that diffraction spikes are a major problem.

There are many other applications, some requiring minor modifications to the existing hardware. These include new time series modes, nod & shuffle imaging, mask & shuffle imaging, broad–narrow switching, tunable polarimetric imaging (Bland-Hawthorn 2000) and tunable echelle imaging (Baldry & Bland-Hawthorn 2000). Further discussion must wait till another time.

1. TECHNICAL PAPERS RELATING TO TUNABLE FILTERS

Review on tunable filters: Bland-Hawthorn (2000, 2001), Bland-Hawthorn et al. (2001).

TTF instrument summary: Bland-Hawthorn & Jones (1998b; 1999), Jones & Bland-Hawthorn (1998), Jones (2001a).

Charge shuffle modes: Bland-Hawthorn & Barton (1995), Glazebrook & Bland-Hawthorn (2001), Maloney & Bland-Hawthorn (2001), Jones (2001b).

TTF data analysis: Joneset al. (2002*b*).

As always in Spanish meetings, the social (and degustatory) calendar was every bit as rewarding as the conference. I am grateful to my longstanding Spanish and Mexican colleagues for interactions sustained by cafés corto, cortado, carajillo, con leche, con gotas, asturias, americano, mediano, desgraciado, and others now forgotten.

REFERENCES

Abraham, R. G., et al. 1999, MNRAS, 303, 641
Alexander, T., et al. 2000, ApJ, 536, 710
Baker, J. C., et al. 2001, AJ, 121, 1821
Baldry, I. K., & Bland-Hawthorn, J. 2000, PASP, 112, 1112
Baldwin, J. A., Phillips, M. N., & Terlevich, R. 1981, PASP, 93, 5
Beauchamp, D., & Hardy, E. 1997, AJ, 113, 1666
Bessell, M. 2001, in Encyclopaedia of Astronomy & Astrophysics, ed. P. G. Murdin (Bristol: IOP Publ. & Macmillan Publ.), 1
Bica, E., et al. 1990, MNRAS, 242, 241
Birkinshaw, M., Worrall, D. M., & Hardcastle, M. J. 2001. In New Visions of the X-ray Universe, ESTEC, in press
Bland-Hawthorn, J. 2000, In ASP Conf. Ser., 195, Imaging the Universe in Three Dimensions, ed. W. van Breugel, & J. Bland-Hawthorn (San Francisco: ASP), 34
Bland-Hawthorn, J. 2001, in Encyclopaedia of Astronomy & Astrophysics, ed. P. G. Murdin (Bristol: IOP Publ. & Macmillan Publ.), 1
Bland-Hawthorn, J., & Barton, J. 1995, AAO Newsletter, 75, 8
Bland-Hawthorn, J., & Jones, D. H. 1998a, PASA, 15, 44
Bland-Hawthorn, J., & Jones, D. H. 1998b, SPIE, 3355, 855

Science with the GTC 10-m Telescope (Granada, España, 5-8 febrero 2002)
Editors: José Miguel Rodríguez Espinosa, Francisco Garzón López & Verónica Melo Martín

Bland-Hawthorn, J., et al. 2001, ApJ, 563, 611
Bowyer, S., Berghöfer, T. W., & Korpela, E. J. 1999, ApJ, 526, 592
Brunthaler, A., et al. 2002, in Proc. 6th European VLBI Network Symposium, ed. E. Ros, R. W. Porcas, & J. A. Zensus (astro-ph/0206185)
Burstein, D., et al. 1984, ApJ, 287, 586
Cecil, G., et al. 2000, ApJ, 536, 675
Cecil, G., et al. 2001, BAAS, 199, 5011
Cecil, G. ,et al. 2002, ApJ, 568, 627
Cepa, J., et al. 2000, SPIE, 4008, 623
Cepa, J., et al. 2002, in Galaxies: The Third Dimension, ed. M. Rosada, L. Binette, & L. Arias, in press
Cianci, S. 2000, AAO Newsletter, 94, 3
Cianci, S. 2002, PhD Thesis, Univ. Sydney
Cianci, S., et al. 2000, in ASP Conf. Ser., 195, Imaging the Universe in Three Dimensions, ed. W. van Breugel & J. Bland-Hawthorn (San Francisco: ASP), 601
Clarke, F., Tinney, C. G., & Covey, K. R. 2002, MNRAS, 332, 361
Collins, J., & Rand, R. 2001, ApJ, 551, 57
Couch, W. J., & Newell, E. B. 1984, ApJS, 56, 143
Couch, W. J., et al. 2001, ApJ, 549, 820
Dalcanton, J. J. 1996, ApJ, 466, 92
Deutsch, E. W., et al. 1998, PASP, 110, 912
Dressler, A., & Gunn, J. E. 1983, ApJ, 270, 7
Dyson, F. 1999, Nat, 400, 27
Ferguson, A., van der Hulst, T., & van Gorkom, J. 2001, AAO Newsletter, 96,4
Francis, P., Wilson, G. M., & Woodgate, B. E. 2001, PASA, 18, 64
Francis, P., et al. 2001, ApJ, 554, 1001
Glazebrook, K. 1997, In Extragalactic Astronomy in the Infrared, ed. G. A. Mamon & T. X Thuan (Moriond), 467
Glazebrook, K., & Bland-Hawthorn, J. 2001, PASP, 113, 197
Gunn, J. E., et al. 1998, AJ, 116, 3040
Heckman, T. 2002, in ASP Conf. Ser., 254, Extragalactic Gas at Low Redshift, ed. J. S. Mulchaey & J. T. Stocke (San Francisco: ASP), 292
Hewett, P. C., et al. 2000, in ASP Conf. Ser., 195, Imaging the Universe in Three Dimensions, ed. W. van Breugel & J. Bland-Hawthorn (San Francisco: ASP), 94
Higdon, J. L., et al. 1997, BAAS, 191, 8907
Hu, E. M., & McMahon, R. G. 1996, Nat, 382, 231
Jaffe, W., & Bremer, M. 2000, AAO Newsletter, 93, 3
Jones, D. H., & Bland-Hawthorn, J. 1998, PASP, 110, 1059
Jones, D. H., & Bland-Hawthorn, J. 1999, in Looking Deep in the Southern Sky, ed. R. Morganti & W. J. Couch (:), 320
Jones, D. H. 2001a, PASP, 113, 255
Jones, D. H. 2001b, in Scientific Drivers for ESO Future VLT/VLTI Instrumentation, ed. J. Bergeron & G. Monnet (Berlin: Springer), in press
Jones, D. H., & Bland-Hawthorn, J. 2001, ApJ, 550, 593
Jones, D. H., Renzini, A., Rosati, P., & Seifert, W. 2001, ESO Messenger, 103, 10
Jones, D. H., Stappers, B., & Gaensler, B. 2002a, A&A, 389, L1
Jones, D. H., et al. 2002b, MNRAS, 329, 759
Kewley, L. J., et al. 2001, ApJ, 556, 121
Knapp, J. 1999, in ASP Conf. Ser., 163, Star Formation in Early-type Galaxies (San Francisco: ASP), 119
Lehnert, M. D., & Heckman, T. M. 1996, ApJ, 462, 651
Lieu, R., et al. 1999, ApJ, 527, L27
Maloney, P. R., & Bland-Hawthorn, J. 2001, ApJ, 553, L129
Meurer, G., et al. 1999, BAAS, 194, 501
Miller, S. T. 2002, PhD Thesis, Univ. Maryland
Miller, S. T., & Veilleux, S. 1999, AAO Newsletter, 88, 4
Miralde-Escudè, J., & Lehar, J. 1992, MNRAS, 259, 31P
Molla, M., Hardy, E., & Beauchamp, D. 1999, ApJ, 513, 695
Offer, A., & Bland-Hawthorn, J. 1998, MNRAS, 299, 176
Pettini, M., et al. 2001, ApJ, 554, 981
Phillips, M. M., et al. 1984, Nat, 310, 554
Pier, E. A., & Krolik, J. H. 1993, ApJ, 418, 673
Pogge, R. W. 1988, ApJ, 328, 519
Reynolds, R., Haffner, M., & Tufte, S. 1999, ApJ, 525, L21
Ryder, S. 2001, AAO Newsletter, 98, 11
Schuberth, Y., & Burton, M. G. 2000, AAO Newsletter, 92, 3
Shopbell, P. L., & Bland-Hawthorn, J. 1998, ApJ, 493, 129
Shopbell, P. L., et al. 1999, ApJ, 524, L83
Shopbell, P. L., et al. 2001, BAAS, 198, 5706
Smail, I., et al. 1998, MNRAS, 293, 124
Sokolowski, J. 1993, PhD, Rice University
Solorzano-Inarrea, C., et al. 2002, MNRAS, 331, 673
Strickland, D. K., & Stevens, I. R. 2000, MNRAS, 314, 511
Tadhunter, C. N., & Tsvetanov, Z. 1989, Nat, 341, 422
Tadhunter, C. N., et al. 2000, MNRAS, 314, 849
Thommes, E., et al. 1998, MNRAS, 293, L6
Tinney, C. G., & Tolley, A. J. 1999, MNRAS, 304, 119
Tresse, L., Maddox, S. J., Le Fevre, O., & Cuby, J.-G. 2001, MNRAS, in press (astro-ph/0111390)
Tresse, L., et al. 2002, MNRAS, in press
van Gorkom, J. 1997, in ASP Conf. Ser., 116, The Nature of Elliptical Galaxies, M. Arnaboldi, G. S. Da Costa, & P. Saha (San Francisco: ASP), 363
Vazdekis, A. 1999, ApJ, 513, 224
Veilleux, S. 2002a, in IAU Coll. 184, AGN Surveys (Dordrecht: Reidel), in press
Veilleux, S. 2002b, in ASP Conf. Ser., 254, Extragalactic Gas at Low Redshift, ed. J. S. Mulchaey & J. T. Stocke (San Francisco: ASP), 313
Veilleux, S. 2002c, in Galaxies: The Third Dimension,

ed. M. Rosada, L. Binette, & L. Arias, in press
Veilleux, S., & Bland-Hawthorn, J. 1997, ApJ, 479, L105
Veilleux, S., & Osterbrock, D. E. 1987, ApJS, 63, 295
Veilleux, S., & Rupke, D. 2002, ApJ, 565, L63
Veilleux, S., et al. 2002, Rev. Mex. Astron. Astrophys., 13, 222
Young, A. J., Wilson, A. S., & Shopbell, P. L. 2001, ApJ, 556, 6
Zaritsky, D., et al. 1997, ApJ, 480, L91
Zurita, A. 2001, PhD Thesis, Univ. La Laguna
Zurita, A., et al. 2000, A&A, 363, 9

J. Bland-Hawthorn: Anglo–Australian Observatory, PO Box 296, Epping, NSW 2121, Australia (jbh@aao.gov.au)